Estimation of Atmospheric Energetics in the Frequency Domain during the FGGE Year

JIAN SHENG*

Program in Atmospheric and Oceanic Sciences, Princeton University, Princeton, New Jersey

YOSHIKAZU HAYASHI

Geophysical Fluid Dynamics Laboratory/NOAA, Princeton, New Jersey

(Manuscript received 22 August 1988, in final form 22 November 1989)

ABSTRACT

The energetics of atmospheric motions are studied in the frequency domain using the two versions of the FGGE IIIb dataset, processed at GFDL and ECMWF. It is demonstrated that the frequency spectra of kinetic energy (KE) and available potential energy (APE) can be approximated by a power law. On a log–log diagram, a slope of minus one results for both KE and APE in the period range of 7 to 35 days, when integrated over the Northern Hemisphere.

The conversion from APE to KE is the major source of eddy kinetic energy for all the low and high frequency bands discussed. Through nonlinear interactions, motions of high frequencies (with periods shorter than 10 days) gain APE from, and lose KE to the motions of low frequencies (with periods longer than 10 days but shorter than the annual cycle). The nonlinear energy exchanges are relatively more important for the energy balance of low frequency modes. It is also shown that both high and low frequency transients extract APE from and supply KE to the time-mean flow. The intercomparisons between the two versions of FGGE data indicate an overall agreement between the energy cycles derived from the GFDL and ECMWF datasets, despite the differences in calculated values of spectral estimates.

1. Introduction

Early in his study of the general circulation, Lorenz (1955) introduced the concept of available potential energy (APE) in discussing the flow of atmospheric energy. He partitioned kinetic energy (KE) and available potential energy into zonal and eddy components and formulated equations governing their mutual exchange. This energy partition permitted a meaningful physical interpretation of the atmospheric energy cycle (e.g., Oort 1964; Lorenz 1967; Hayashi 1987). The energetic role of atmospheric disturbances has been studied extensively. The wavelike nature of the global distribution of the wind and temperature suggests the appropriateness of a further decomposition of KE and APE into a spectrum of spatial scales by one-dimensional Fourier analyses around latitude circles (Saltzman 1957). Decomposition of the total energy into barotropic and baroclinic components has been proposed by Wiin-Nielsen (1962). Chen and Wiin-Nielsen (1976) studied the energy conversion between divergent and nondivergent flows based upon the primitive equations. Recently, energy decomposition was further pursued in terms of three-dimensional normal mode functions by Tanaka (1985).

Low frequency motions in the atmosphere have attracted special attention in the meteorological community in recent years. The term "low frequency" is used here to distinguish this class of disturbances from the synoptic systems of relatively high frequency (periods 1 to 10 days) and from those of annual or interannual time scales. In the middle latitudes, Blackmon et al. (1977) observed that the principal storm tracks over the oceans coincided with sites of elongated maxima in the variance of band-pass filtered (periods 2.5–6 days) geopotential height fields at the jet stream level, where baroclinic wave activity is most intense. However, regions of frequent blocking corresponded closely to the variance maxima of low-pass filtered data (periods longer than 10 days) located over the North Atlantic and Pacific oceans and over the Siberian Arctic. Furthermore, simultaneous and lagged correlation maps suggested that the band-pass filtered data were characterized by wavelike fluctuations in the upper level flow with wavelengths on the order of 4000 km. Similar maps with low-pass filtered data, however, indicated geographically fixed patterns, most notably, the PNA (Pacific–North America) pattern (Blackmon et al. 1984a,b). Theoretical work on Rossby wave dis-

* Present affiliation: Department of Meteorology, McGill University, Montreal, Canada.

Corresponding author address: Dr. Jian Sheng, Dept. of Meteorology, McGill University, 805 Sherbrooke Street West, Montreal, Quebec, Canada H3A 2K6.

persion along a great circle on a sphere provides a basis for interpreting these correlation patterns as resulting from wave trains with a ray path starting in the tropics, turning eastward to become tangent to a latitude circle, and curving back into the tropics. Such wave trains constitute the response of the atmosphere to a sustained geographically localized forcing (Hoskins and Karoly 1981). Low frequency oscillations of great interest are also found in the tropics. Madden and Julian's work (1971, 1972), dealing with the equatorial sea level pressure field and zonal wind clearly demonstrated a dominant mode of a 40–50 day period. They showed that these low frequency oscillations are primarily associated with changes in the zonal component of the wind, but with a phase speed different from theoretical Kelvin waves. Yasunari (1980, 1981) emphasized the relationship between the low frequency oscillations and the Northern Hemisphere summer monsoon. Krishnamurti et al. (1985) noted a zonal propagation of divergent waves at 200 mb with a maximum amplitude in the middle latitudes throughout the FGGE year.

From these studies it is evident that fluctuations with periods longer than about 10 days exhibit a structure and evolution quite different from their high frequency counterparts. It has been widely accepted that baroclinic instability is energetically the main source of synoptic disturbances found in the general circulation. From the view of energetics, time scales of these low frequency motions are so long that the classical theory of linear baroclinic instability is no longer valid. It is therefore of interest to investigate the energetics of the atmospheric transients as a function of time scale. Energetics in the wavenumber domain (Saltzman 1957; 1970) utilize a decomposition according to spatial scales. However, spectral analyses in space and/or time by Vinnichenko (1970), Wilson (1975), and Hayashi and Golder (1977) indicated there was no simple relationship between the kinetic energy spectra in the wavenumber and frequency domains. The scheme proposed by Hayashi (1980) decomposes meteorological time series into Fourier components so that energy conversions can be viewed through spectral windows of different frequency ranges. The present study, to our knowledge, is the first attempt to make a comprehensive documentation of atmospheric energetics in the frequency domain. In section 2, the formulation of energetics in the frequency domain is briefly reviewed. The datasets used in this study are discussed in section 3. The remainder of this paper is devoted to discussions of the energy cycle in the frequency domain and the contrast between different datasets.

2. Scheme of analysis

The formulation of energy equations in the frequency domain was discussed by Hayashi (1980) and Sheng (1986). The APE equation used in the present study, however, is a variation of Hayashi's (1980) scheme. A brief derivation is presented in appendix A for reference. First, definitions of $K(n)$ and $A(n)$, the KE and APE associated with frequency f_n, are given as

$$K(n) = \frac{1}{2}[P_n(u, u) + P_n(v, v)], \quad n \geq 0 \tag{1}$$

$$A(n) = \begin{cases} \dfrac{\gamma}{2} P_n(\theta, \theta) & n \geq 1 \\ \dfrac{\gamma}{2} P_n(\theta^*, \theta^*). & n = 0 \end{cases} \tag{2}$$

A list of symbols, definitions, and variables is given in appendix B. For $K(n)$ and $A(n)$ the energy equations may be written as,

$$0 = \langle K(m)\cdot K(n)\rangle + \langle K(0)\cdot K(n)\rangle + \langle A(n)\cdot K(n)\rangle + F(n) - D(n) \tag{3}$$

and

$$0 = \langle A(m)\cdot A(n)\rangle + \langle A(0)\cdot A(n)\rangle - \langle A(n)\cdot K(n)\rangle + G(n), \tag{4}$$

where

$$\langle A(n)\cdot K(n)\rangle = -P_n(\omega, \alpha), \tag{5}$$

$$F(n) = -g\left[\frac{\partial}{\partial x} P_n(u, z) + \frac{\partial}{\partial y} P_n(v, z) + \frac{\partial}{\partial p} P_n(\omega, z)\right], \tag{6}$$

$$G(n) = \gamma\left[\frac{\theta}{C_p T}\right] P_n(\theta, h), \tag{7}$$

$$D(n) = -[P_n(u, F_u) + P_n(v, F_v)], \tag{8}$$

$$\begin{aligned}\langle K(m)\cdot K(n)\rangle = &-\left[P_n\left(u, \frac{\partial}{\partial x} u'u'\right) + P_n\left(u, \frac{\partial}{\partial y} v'u'\right)\right. \\ &+ P_n\left(u, \frac{\partial}{\partial p} \omega'u'\right) + P_n\left(v, \frac{\partial}{\partial x} u'v'\right) \\ &\left. + P_n\left(v, \frac{\partial}{\partial y} v'v'\right) + P_n\left(v, \frac{\partial}{\partial p} \omega'v'\right)\right] \\ &+ \frac{\tan\phi}{a}[P_n(u, u'v') - P_n(v, u'u')],\end{aligned} \tag{9}$$

$$\begin{aligned}\langle K(0)\cdot K(n)\rangle = &-\left[P_n\left(u, \frac{\partial}{\partial x} uu\right) + P_n\left(u, \frac{\partial}{\partial y} vu\right)\right. \\ &\left. + P_n\left(u, \frac{\partial}{\partial p} \omega u\right) + P_n\left(v, \frac{\partial}{\partial x} uv\right)\right.\end{aligned}$$

$$+ P_n\left(v, \frac{\partial}{\partial y} vv\right) + P_n\left(v, \frac{\partial}{\partial p} \omega v\right)\Big] + \frac{\tan\phi}{a}\left[P_n(u, uv) - P_n(v, uu)\right] - \langle K(m)\cdot K(n)\rangle, \quad (10)$$

$$\langle A(m)\cdot A(n)\rangle = -\gamma\Big[P_n\left(\theta, \frac{\partial}{\partial x} u'\theta^{*\prime}\right) + P_n\left(\theta, \frac{\partial}{\partial y} v'\theta^{*\prime}\right) + P_n\left(\theta, \frac{\partial}{\partial p} \omega'\theta^{*\prime}\right)\Big], \quad (11)$$

and

$$\langle A(0)\cdot A(n)\rangle = -\gamma\Big[P_n\left(\theta, \frac{\partial}{\partial x} u\theta^{*}\right) + P_n\left(\theta, \frac{\partial}{\partial y} v\theta^{*}\right) + P_n\left(\theta, \frac{\partial}{\partial p} \omega\theta^{*}\right)\Big] - \langle A(m)\cdot A(n)\rangle. \quad (12)$$

These terms are interpreted as follows:

$\langle A(m)\cdot A(n)\rangle$	Transfer of APE into frequency f_n by nonlinear interactions of transient disturbances.
$\langle A(0)\cdot A(n)\rangle$	Transfer of APE into frequency f_n from the time mean flow.
$\langle A(n)\cdot K(n)\rangle$	Baroclinic conversion from APE to KE at frequency f_n.
$\langle K(m)\cdot K(n)\rangle$	Transfer of KE into frequency f_n by nonlinear interactions of transient disturbances.
$\langle K(0)\cdot K(n)\rangle$	Transfer of KE into frequency f_n from the time mean flow.
$F(n)$	Convergence of energy flux associated with frequency f_n.
$G(n)$	Generation of APE associated with frequency f_n.
$D(n)$	Dissipation of KE associated with frequency f_n.

In Eqs. (5)–(12) the estimations of energy conversions involve the use of frequency cross spectra, which are computed by the Fourier transform method discussed in Madden and Julian (1971).

3. Data preparation

The datasets used are the Level IIIb data from the First GARP (Global Atmospheric Research Program) Global Experiment (FGGE), processed at the Geophysical Fluid Dynamics Laboratory (GFDL) with a FGGE data assimilation system (see Miyakoda et al. 1982), and by the European Centre for Medium Range Weather Forecasts (ECMWF) with a slightly modified version of the operational assimilation system (Bengtsson et al. 1982). For both datasets the period covers the entire FGGE year from 1 December 1978 to 30 November 1979. Variables are interpolated onto a grid over the Northern Hemisphere with 25 latitudes and 64 longitudes, corresponding to a 5.625 × 3.75 degree mesh. The datasets contain the once daily standard variables of geopotential height, temperature, wind, and pressure velocity at 100, 200, 300, 500, 700, 850, and 1000 mb levels at 1200 UTC.

It is indicated in the FGGE III-b data manual that caution should be taken in using temperature and vertical velocity fields generated by the ECMWF analyses. In a preliminary test, the rate of baroclinic conversion was calculated with kinematic velocity and temperature derived from the hydrostatic relationship, and the results were compared with the rate calculated from the original temperature and vertical velocity. For a 10-day period tested, the difference was minor between the hemispherically averaged values (less than 4 percent for each of the 10 days). In order to make close comparisons between the GFDL and ECMWF datasets, it was decided to use the original ECMWF temperature and vertical velocity fields throughout this study.

In Eqs. (3) and (4), the generation of available potential energy and the dissipation of kinetic energy are obtained as residual terms to balance the respective equations after the other terms are evaluated from the data.

4. Spectral distributions of APE and KE

Figure 1 shows the spectra of available potential energy $A(n)$ and kinetic energy $K(n)$ as functions of frequency after integrations over the mass of the Northern Hemisphere for the GFDL data. The abscissa corresponds to the logarithm of frequency and the ordinate to the energy density multiplied by the frequency, following Zangvil (1977). The areas under the curves are proportional to the transient energy, and the units are in J m^{-2}. The most noticeable feature of the spectral APE is a pronounced peak at the period of one year, which contains about 70 percent of the transient APE. Toward higher frequencies no significant energy peak can be found, except for a broad maximum around the period of 10 days. The spectrum of kinetic energy indicates a very similar distribution, although the transient KE of the annual cycle is only 20 percent of the total variance.

If the APE spectrum is further separated into zonal and eddy parts, it is easy to see that almost the entire APE of the annual cycle resides in the zonal part, with the ratio of zonal APE to eddy APE roughly 7 to 1. At the high frequency end, the opposite is true, with a negligible ratio of less than 1 to 30 (Fig. 2). On the other hand, as shown in Fig. 3, kinetic energy has less contrast at the annual time scale, with the ratio of zonal KE to eddy KE roughly 2 to 1. At high frequencies, however, this ratio drops down to less than 1 to 50.

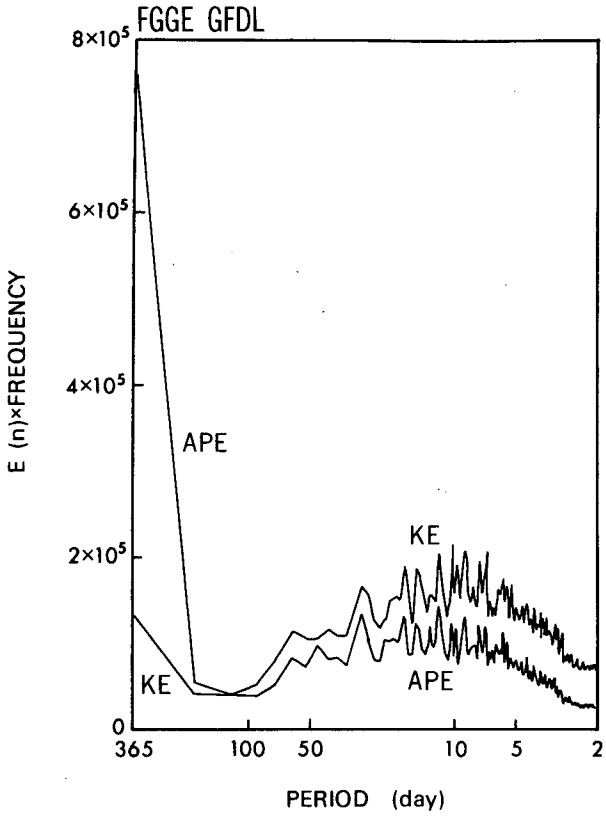

FIG. 1. Spectral distributions of APE and KE for the GFDL data. The abscissa is frequency in a log-scale with the Nyquist frequency equal to 0.5 day^{-1}. The ordinate is energy density multiplied by the frequency, in units of J m^{-2}.

These features clearly indicate that both APE and KE residing in the annual cycle are associated mostly with zonally symmetric fields, while energy with higher frequencies is characterized by zonally asymmetric disturbances of smaller scales.

Figure 4 shows the spectral APE and KE on a log–log scale. Both spectra have a slope of approximately minus one (-1) for frequencies far removed from the annual cycle and from the high frequency end. A least square fit of the KE spectrum gives a slope of -1.13 for the period interval from 7 to 35 days. The APE spectrum, on the other hand, follows a slightly steeper slope of approximately -1.19. It is seen that both curves follow the slope of minus one quite well, up to a period of 7 days, where the energy starts to decay at a faster rate. The minus one slope has been previously reported by Vinnichenko (1970), and by Kao and Lee (1977), who used a much shorter time series of 90 days for this frequency range.

There has been considerable interest in the slope of the atmospheric energy spectrum in the high wavenumber regime from both practical and theoretical points of view. Spectra of APE and KE for the extratropics were calculated by Wiin-Nielsen (1967), Julian et al. (1970) and Charney (1971) from a variety of data sources. It was shown in all these investigations that it was possible to write the kinetic energy spectra in the form of

$$K(k) = bk^{-c}, \tag{13}$$

where $K(k)$ is the kinetic energy per unit wavenumber, k the zonal wavenumber, with b and c empirical constants. The value of c as it appears in Eq. (13) has been found to vary between 2.5 and 3.2, depending on the data sample, with a tendency toward a value of 3 for the spectral region $8 \leqslant k \leqslant 16$. A value of $c \sim 3$ has also been found by Manabe et al. (1970) for data generated by a general circulation experiment.

The shape of the kinetic energy spectrum is of interest because it seems to influence the limits of deterministic forecasting (Lorenz 1969; Leith 1971). A second factor that makes the power law of additional importance is that the theoretical investigations by Kraichnan (1967), Leith (1968), and Charney (1971) suggest the observed slope of -3 in the energy spectrum could be evidence for an inertial subrange characterized by a constant flux of enstrophy (one-half of the vorticity squared) and a vanishing flux of energy. In the context of the frequency domain, however, to this point there has been no theoretical attempt to relate the -3 slope in the wavenumber domain to the -1 slope in the frequency domain, and the physical significance of this -1 slope is not clear.

Since the hemispherically mass integrated power spectra are essentially red and show no significant peaks in the frequency range beyond the annual cycle, a different approach is proposed to represent the energy spectra. First, the entire frequency range is divided into frequency bands according to a constant interval of $\log f$,

$$\Delta f_n = f_{n+1} - f_n, \tag{14}$$

where

$$f_{n+1}/f_n = c \quad \text{or} \quad \ln f_{n+1} - \ln f_n = \text{const}. \tag{15}$$

Here c is a constant, independent of n. The energy spectrum within each frequency band is integrated and plotted. The advantages of this technique are the following:

(i) Contributions from each frequency interval are proportional to the energy, rather than the energy density multiplied by frequency, as in Zangvil's diagram.

(ii) Under the exact minus one frequency distribution, each frequency band has the same amount of energy,

$$\int_{f_n}^{f_{n+1}} \frac{A}{f}\, df = A \ln f \Big|_{f_n}^{f_{n+1}} = A \ln \frac{f_{n+1}}{f_n} = \text{const}, \tag{16}$$

where A is a constant. This type of frequency division is actually a generalization of what Lorenz (1979)

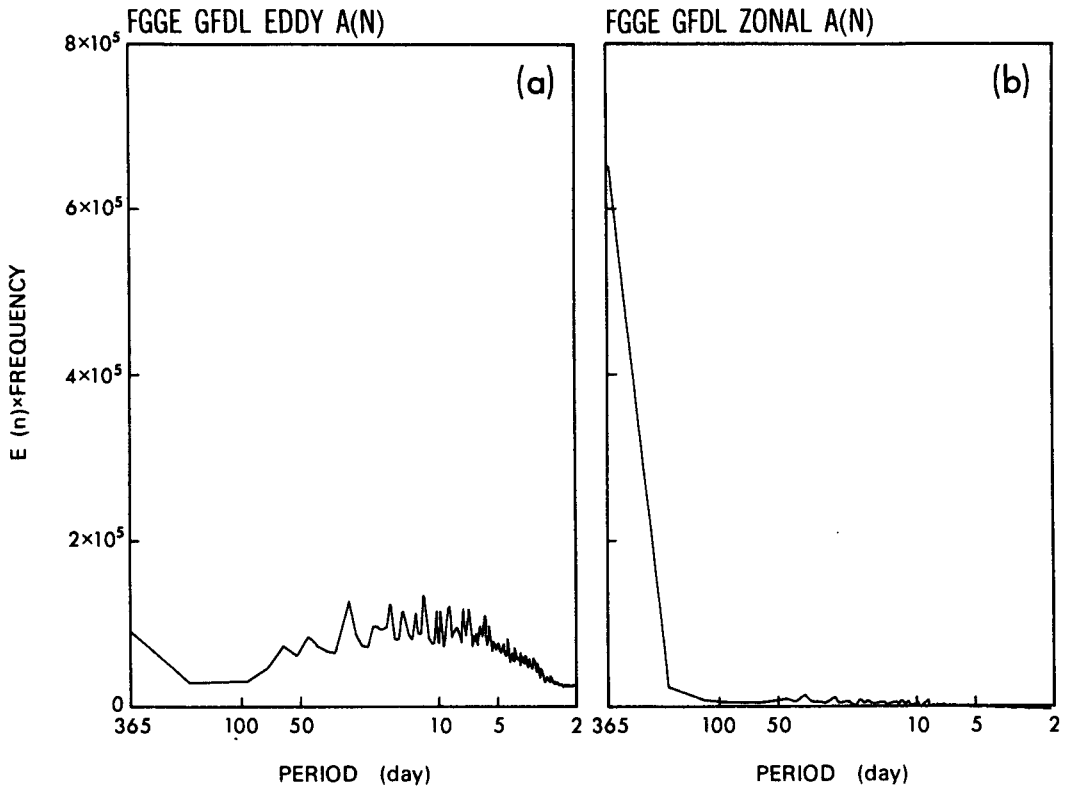

FIG. 2. As in Fig. 1, but for (a) eddy APE, and (b) zonal APE.

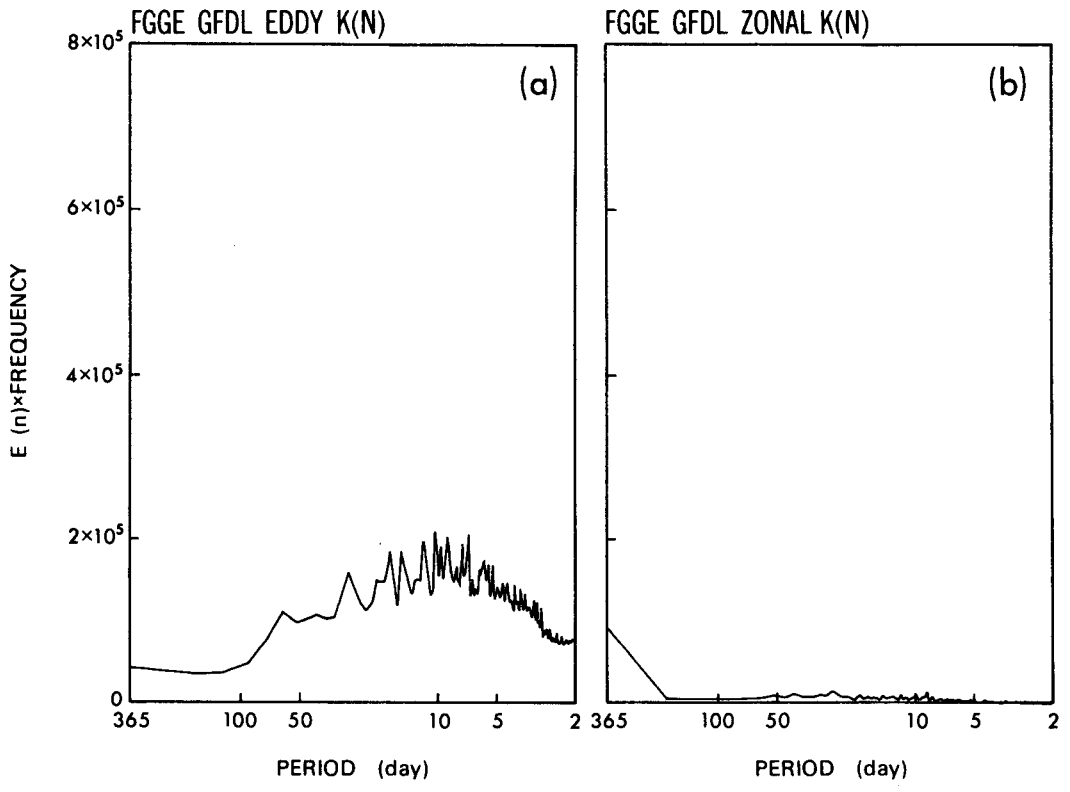

FIG. 3. As in Fig. 1, but for (a) eddy KE, and (b) zonal KE.

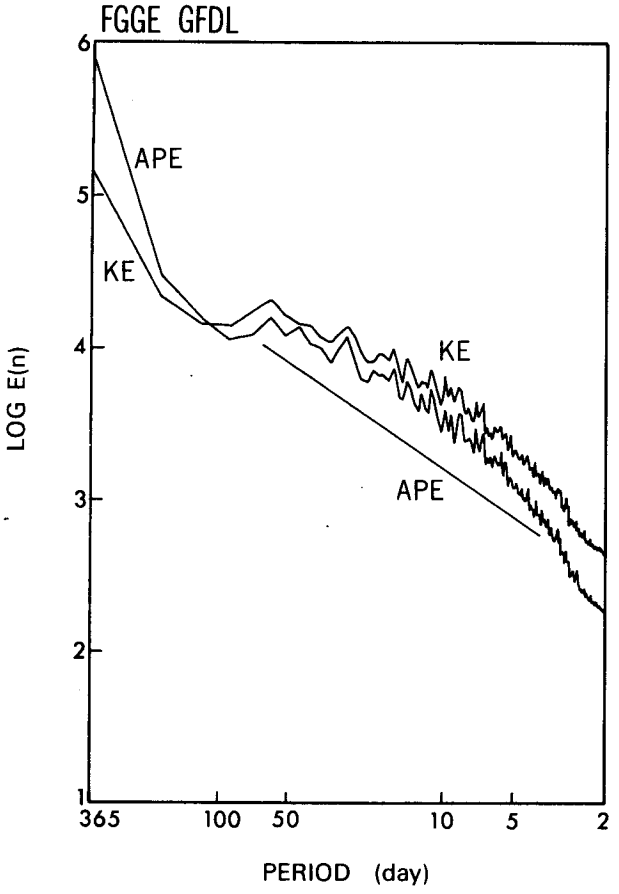

FIG. 4. Spectral distributions of APE and KE for the GFDL data. The abscissa is frequency and the ordinate is energy, both in log-scale. The Nyquist frequency is 0.5 day^{-1}. Also shown is a straight line indicating a minus one slope. (a) APE; (b) KE.

adopted for presentation of his "poor man's spectrum" for which the c in Eq. (15) was taken as 2. Figure 5 shows the spectral distributions of APE (a) and KE (b), where $c = f_{n+1}/f_n$ is chosen as 1.5. The energy of the time mean is also indicated by the leftmost bar. As an indication of the minus one slope, nearly constant levels of APE and KE are observed in the period range from 6.8 to 34 days.

5. Spectral energetics in the frequency domain

Upon integration over the mass of the Northern Hemisphere the KE and APE equations take the form

$$0 = \langle K(m)\cdot K(n)\rangle + \langle K(0)\cdot K(n)\rangle + \langle A(n)\cdot K(n)\rangle - D(n) + \text{boundary flux terms}, \quad (17)$$

$$0 = \langle A(m)\cdot A(n)\rangle + \langle A(0)\cdot A(n)\rangle - \langle A(n)\cdot K(n)\rangle + G(n) + \text{boundary flux terms}. \quad (18)$$

As pointed out by Oort and Peixoto (1974), the boundary flux terms at the equator can be neglected for the annual mean case. In the present study the boundary terms were also found to be negligibly small, and attention is concentrated only on those terms of

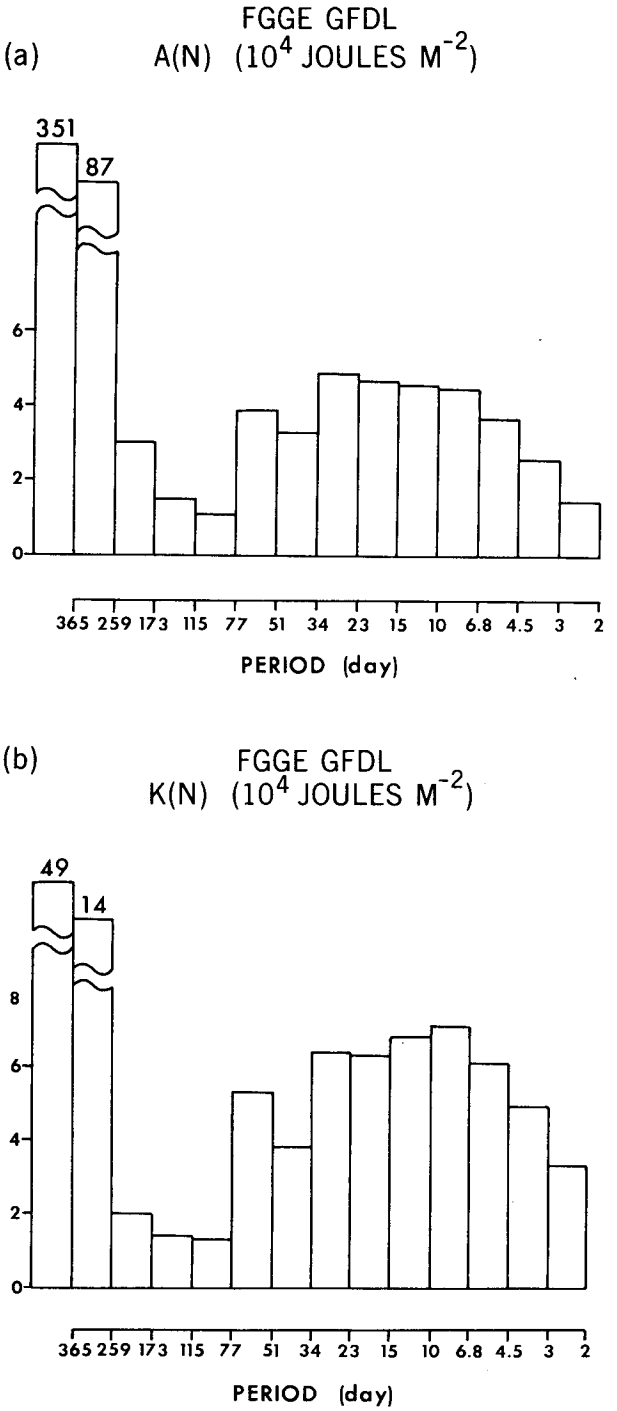

FIG. 5. Spectral distributions of (a) APE, and (b) KE for the GFDL data, plotted with a constant interval of log-frequency. In units of J m^{-2}. The leftmost bar indicates the energy of the time mean.

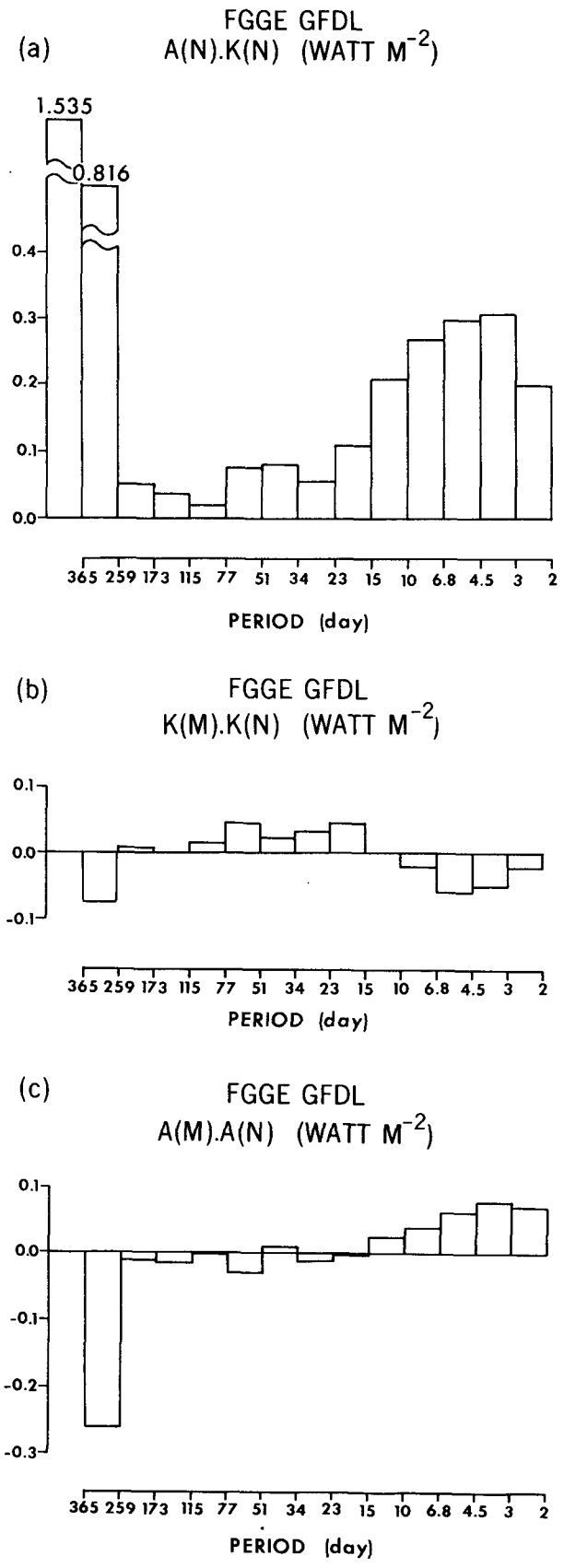

interior contributions. First, estimates of the spectral energetics from the GFDL data are presented.

Figure 6a shows the frequency distribution of $\langle A(n) \cdot K(n) \rangle$; i.e., the conversion from APE to KE. The total conversion (summation over all frequency bands) amounts to 4.101 W m^{-2}, which is in good agreement with the value obtained by Kung (1988) for the FGGE year. Contributions are mostly concentrated in two frequency regions; i.e., the time mean (35 percent) and high frequencies (period shorter than 10 days, 22 percent). It is important to note that the situation is quite different for spectral energetics in the wavenumber domain, where disturbances of high wavenumbers (short waves) are energetically inactive and, therefore, most conversion occurs within the first 10 harmonics (Saltzman 1970). This difference is consistent with the fact that the energy spectrum decays much slower with frequency (-1 slope) than with wavenumber (-3 slope).

The kinetic energy exchange among different frequencies, $\langle K(m) \cdot K(n) \rangle$, is presented in Fig. 6b. Theoretically, the summation over all frequency bands should vanish, however, the numerical value turns out to be 0.03 W m^{-2}. Energy is lost at high frequencies through nonlinear energy exchange, while it is gained at low frequencies, except for the annual cycle. The transition frequency between the regions of energy gain and energy loss corresponds to approximately a period of 10 days. Figure 6c gives the nonlinear APE exchange among different frequencies. Energy is gained at high frequencies and lost at low frequencies. The transition frequency between the gain and loss also corresponds to a period of 10 days as was the case for KE.

To summarize the energy cycle presented above, the energy reservoirs are regrouped as motions of the time mean, annual cycle, low frequency, which represents approximately the frequency range between the synoptic time scale and the annual cycle, and high frequency, which represents the synoptic time scales shorter than 10 days. This grouping is only subjective and is meant to provide a simplified view of the energetics in the frequency domain. The energy cycle is schematically illustrated in Fig. 7. Available potential energy is generated by diabatic processes almost entirely in the components of the time averaged flow and the variations of the annual cycle. Energy flows down to shorter time scales by the eddy heat transfer process measured by $\langle A(0) \cdot A(n) \rangle$ and $\langle A(m) \cdot A(n) \rangle$. Simultaneously, the potential energy is generally reduced by conversion of this potential energy into kinetic energy in all frequency groups. An important part of this conversion occurs in the group of high frequency transients, which corresponds to the unstable disturbances

FIG. 6. Spectral distributions of energy conversions estimated from the GFDL data. In units of W m^{-2}. (a) $\langle A(n) \cdot K(n) \rangle$, the conversion from APE to KE; (b) $\langle K(m) \cdot K(n) \rangle$, the nonlinear exchange of KE; (c) $\langle A(m) \cdot A(n) \rangle$, the nonlinear exchange of APE.

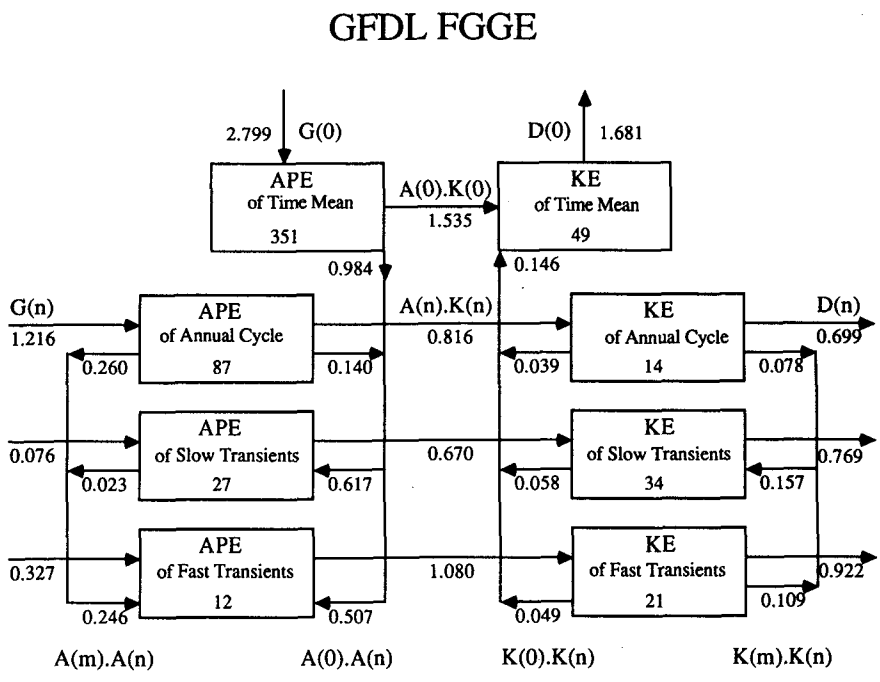

FIG. 7. Schematic depiction of the atmospheric energy cycle in the frequency domain estimated from the GFDL data. Numbers in boxes denote the energy storage in 10^4 J m^{-2}, and fluxes of energy are in W m^{-2}.

predicted by the theory of baroclinic instability. Through the nonlinear momentum transfer process measured by $\langle K(m) \cdot K(n) \rangle$, the kinetic energy flows into the low frequency group, although this contribution is relatively small in comparison with the baroclinic conversion term $\langle A(n) \cdot K(n) \rangle$. A smaller amount of kinetic energy is also transferred into the time-mean flow against frictional dissipation.

To test the sensitivity of the estimates of the energy cycle with respect to the datasets prepared by different four-dimensional assimilation systems, and to provide a confidence limit for this analysis scheme, the spectral energetics of the FGGE year are computed using the ECMWF dataset. The results corresponding to Figs. 5 through 7 are shown in Figs. 8 through 10 for the ECMWF data. It is readily seen that there is an overall agreement in the spectral distributions of APE and KE, despite variations in numerical estimates for several frequency regions shown in Fig. 8 (as compared to Fig. 5). Overall, the frequency bands calculated for the ECMWF analysis indicate a consistently lower level of energy density, usually a difference of 10 percent. In view of the previous intercomparisons of energetics by Kung and Tanaka (1983) for special observational periods of FGGE year, the difference shown in the present study seems reasonable.

In comparing the directions of energy flow in the frequency domain, general agreement between GFDL and ECMWF versions of the FGGE data can be seen. One apparent discrepancy appears for the conversion term $\langle A(n) \cdot K(n) \rangle$ shown in Fig. 6a and 9a. For most frequency intervals the estimates for the ECMWF analysis are 30% smaller than those for the GFDL analysis. More significant differences are found at the annual cycle and the time-mean regions, where the baroclinic conversion of the ECMWF data is only one-third of that of the GFDL data. If the $\langle A(n) \cdot K(n) \rangle$ term is integrated over all the frequency bands, the annual mean values of energy conversion from APE to KE should be recovered. For the GFDL and ECMWF datasets, the results of 4.101 and 1.856 W m^{-2} are obtained, respectively. These values are consistent with the values calculated for the special observational periods of FGGE (Kung and Tanaka 1983).

It is known that the divergent component of the wind in the ECMWF data is underestimated, especially in the tropics. For lack of an independent estimation of spectral energetics in the frequency domain, the discrepancy in the distribution of $\langle A(n) \cdot K(n) \rangle$ is attributed to the different four-dimensional data analysis schemes used at GFDL and ECMWF. The wide difference in the baroclinic conversion rate between the two datasets is also noticed in the energetics of the wavenumber domain (Kung and Tanaka 1983). In a study of meridional circulation, they suggested that this discrepancy is largely due to the contrast between the divergent circulations, particularly the Hadley cells, appeared in the two versions of the analyses. It is therefore important to remember that the energy balance in the annual cycle and time-mean regions are subject

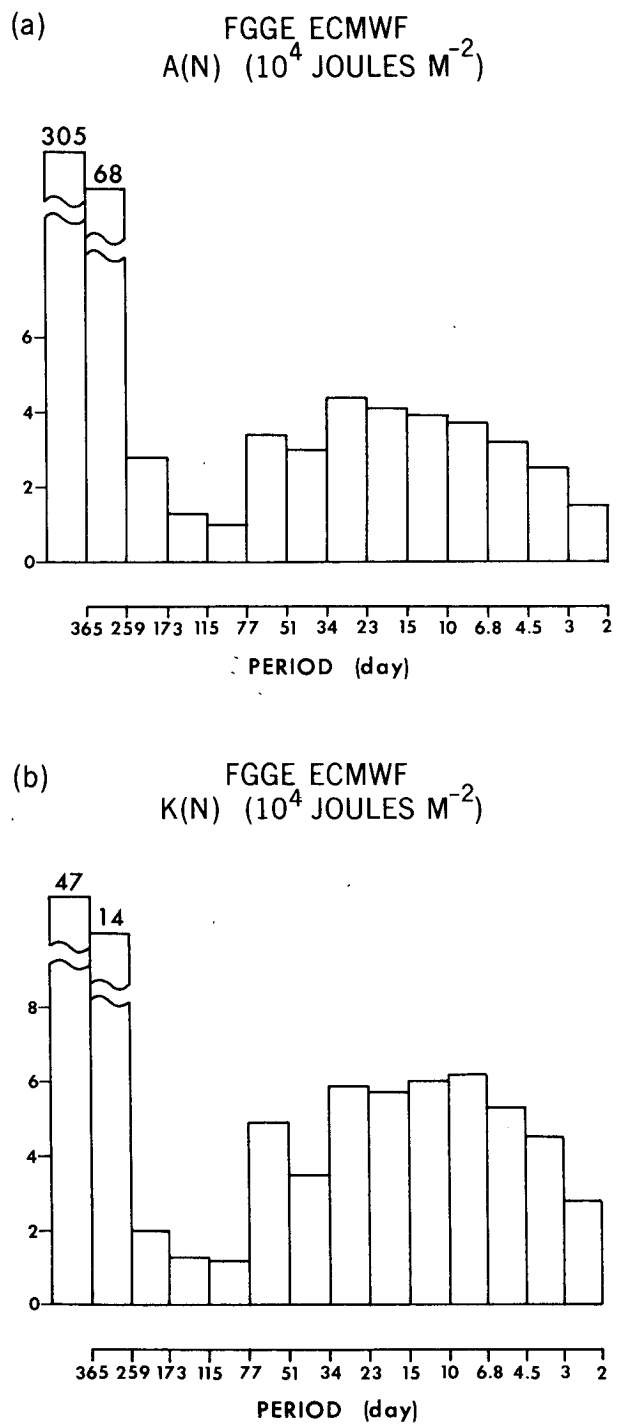

FIG. 8. As in Fig. 5, but for the ECMWF data.

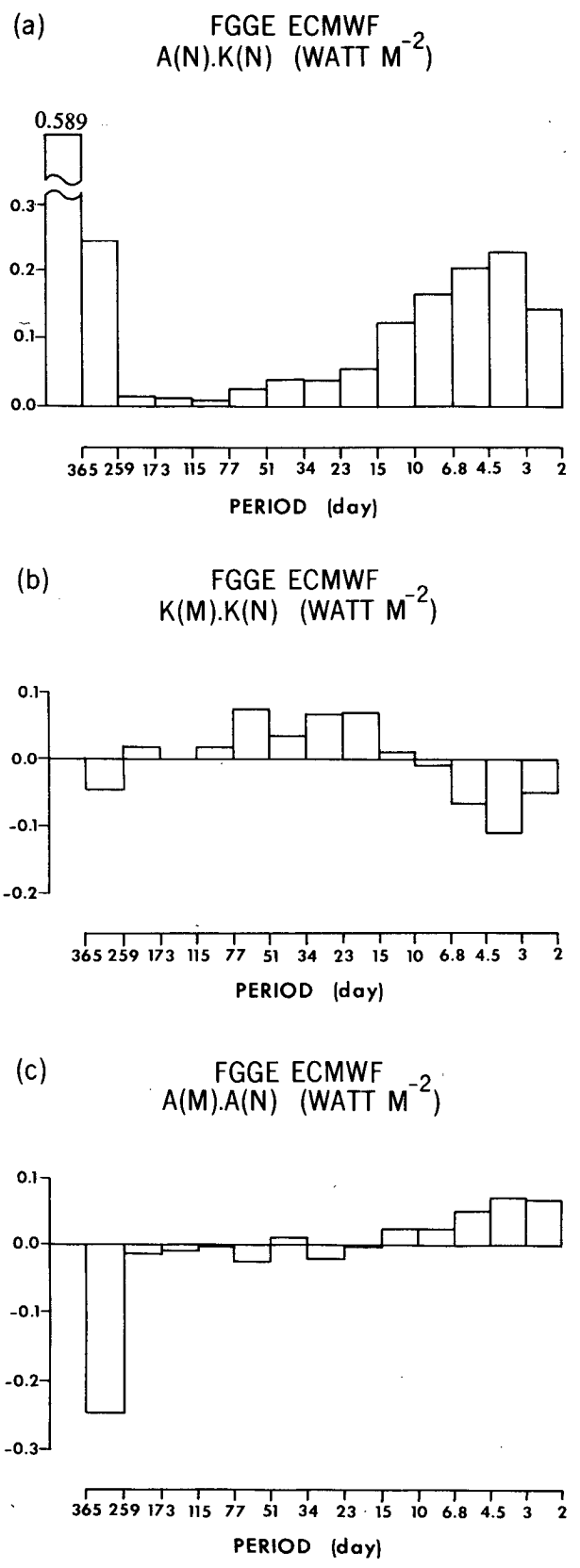

FIG. 9. As in Fig. 6, but for the ECMWF data.

to serious uncertainty due to the inability to make an accurate estimation of $\langle A(n) \cdot K(n) \rangle$. In comparing Fig. 6b with Fig. 9b, attention should be given to the much stronger KE exchange between the fast transients and the slow transients for the ECMWF dataset. Actually, when integrating over the low frequency band

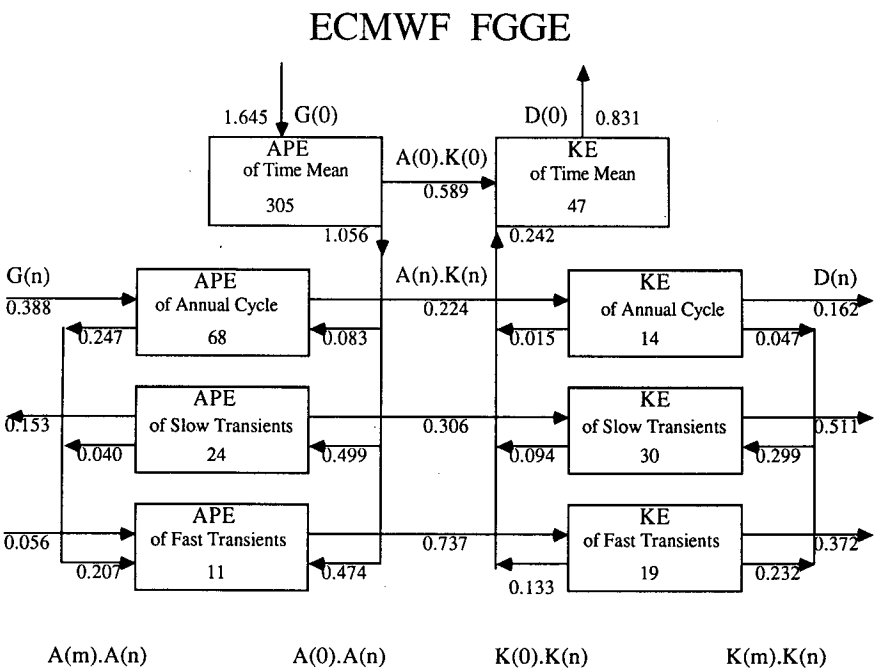

FIG. 10. As in Fig. 7, but for the ECMWF data.

the energy gain is nearly doubled, from 0.157 (GFDL) to 0.299 W m^{-2} (ECMWF). As a consequence of a stronger $\langle A(n) \cdot K(n) \rangle$ and a weaker $\langle K(m) \cdot K(n) \rangle$ for the GFDL data, the nonlinear exchange of KE is comparable in magnitude to the baroclinic conversion from APE to KE for the ECMWF data, in contrast to the GFDL data where $\langle K(m) \cdot K(n) \rangle$ plays a less important role.

In this study the datasets used are both hemispheric and cover the same period, and have been produced from comparable original observations. Moreover, identical data processing and calculation procedure have been applied to estimate the spectral energetics. Consequently any noticeable differences between the energy cycles derived from the GFDL and the ECMWF datasets should be noted as due to the difference in the objective analysis schemes and the four-dimensional assimilation processes involved in preparing these versions of the data.

6. Concluding remarks

The spectral distributions of the hemispheric energy and energy transformation show some very interesting characteristics for the FGGE year. The energy spectra of KE and APE are observed to have no significant energy peak for the entire frequency range other than the annual cycle. Both KE and APE, however, show broad spectral maxima around the frequency of 10 days when the spectra are multiplied by the frequencies. The feature of red energy spectra in the atmosphere should be considered as the background spectra of climatological energy spectra as a function of frequency. On a log–log scale, the energy spectra of KE and APE decay with frequency, having a nearly constant slope of approximately minus one for the frequency range between the 7- and 35-day periods. The latitude–pressure variation of this slope was studied by Sheng (1986) using a 5-year dataset from the ECMWF. Although the slope varies significantly as a function of latitude and pressure, the value of minus one may be considered as representative for the midlatitude troposphere. Since the study of Kraichnan (1967), it has been recognized that a minus three slope for the KE spectrum in the wavenumber domain is an indication of the existence of an inertial subrange for two dimensional turbulence. However, a theoretical explanation for the minus one slope in the frequency domain is not known at this time.

The transient fluctuations have been conveniently divided into low frequency and high frequency (synoptic time scale) groups at the time scale of 10 days. The 10-day period is chosen because the nonlinear exchanges of KE and APE both change sign near this frequency. This grouping is somewhat arbitrary but seems physically sound for the purpose of interpreting the energy cycle. The group of high frequency disturbances shows an energy cycle very similar to the classic diagram given by Oort (1964). Namely, the mean differential heating generates the time-mean APE and the baroclinic transient disturbances transform the time-mean APE into the synoptic scale APE. At the same time the transient APE is converted into transient KE by the vertical motions having a synoptic time scale;

the KE of the time-mean flow is maintained by the transients through the barotropic conversion of KE.

The following remarks on maintenance of low frequency disturbances need to be stressed:

1) The importance of baroclinic energy conversion in maintenance of low frequency variations has been demonstrated. This is somewhat surprising, since low frequency motions are observed to have an equivalent barotropic vertical structure, and therefore, are commonly thought to involve a smaller conversion of energy from APE to KE. However, the observational study by Krishnamurti et al. (1985) for the FGGE year showed evidence of strong baroclinic energy conversion for the 30 to 50 day filtered disturbances. The results from the GCM simulation studied in Hayashi and Golder (1983) indicate that baroclinic energy conversion is the primary energy source for low frequency oscillations in the extratropics. It is clear from our calculation that baroclinic conversion is energetically important not only for disturbances of the synoptic time scale but also for the slow transients. Although a difference in total conversion from APE to KE is observed in the two versions of FGGE data, it is believed that the uncertainty is mostly restricted to the motions of the time mean and the annual cycle and therefore the importance of $\langle A(n) \cdot K(n) \rangle$ relative to other energy conversion terms is established.

2) The present study suggests strong evidence of a kinetic energy supply from the fast transients into the slow transients. This kind of energy "decascade" is viewed as a barotropic enhancement of low frequency variability by nonlinear interactions with the high frequency eddies. The synoptic case study of blocking ridges by Green (1977) provides a substantiation of such a notion in the real time frame. Recently, Mullen (1987) studied the transient eddy forcing of blocking flows and found that anticyclonic eddy forcing is located about one-quarter of a wavelength upstream of the blocking anticyclone. Other investigations of cyclone scale activities during selected blocking events include Illari (1984), Dole (1986), and Holopainen and Fortelius (1987). Lau (1988) showed that vorticity transport by cyclone-scale eddies act to reinforce the monthly mean anomalies. It is helpful to recognize that the present energetics approach, which is based on continuous time series, diagnoses the statistical relationship between the high frequency and the low frequency oscillations while the case study approach is focused only on a selected class of atmospheric phenomena such as blocking events. Fast transients, on the other hand, are enhanced through the nonlinear APE cascade. Lau and Holopainen (1984) studied the geopotential tendency distributions and found that the forcing at the 300 mb level due to the transient heat transport is opposite to, but considerably weaker than, the forcing due to eddy vorticity transport. However, since the eddy forcing at lower levels such as 850 mb is dominated by eddy heat fluxes, the present investigation indicates that the loss of APE in the low frequency region due to the dissipation effects of high frequency eddies cannot be ignored. Similar features were also documented by Savijarvi (1977).

3) The role of the time-mean flow on low frequency transients has been a renewed topic in recent years with the traditional concept of "baroclinic instability" and "barotropic stability," as termed by Smagorinsky (1972) being challenged by recent investigations. Simmons et al. (1983) showed evidence that barotropic instability of the wintertime climatological mean flow plays a role in several observed patterns of low frequency eddies. The primary mechanism by which the unstable normal modes extract kinetic energy from the time-mean flow is through the eastward (downgradient) flux of zonal momentum in the jet-exit regions. The characteristics associated with this instability are fundamentally different from those associated with the classic barotropic instability problem of zonally symmetric flow studied by Kuo (1949). Wallace and Lau (1985), using several observed and model simulated datasets, calculated the barotropic conversion term and examined the interactions between the transient eddies and the longitudinally dependent mean flow. It was shown that the high frequency transients feed kinetic energy into the mean flow at the jet stream level, while low frequency transients extract kinetic energy from this mean flow. There is a strong compensation between the high and low frequency fluctuations such that the conversions for the time filtered eddies are about an order of magnitude larger than the net rate of conversion for the transient eddies as a whole. As indicated in Figs. 7 and 10, the positive barotropic energy conversion in the low frequency region appears in neither of the datasets that have been analyzed, although the magnitudes are smaller compared with the high frequency region. It is speculated that the discrepancy between the earlier and present studies is due largely to the fact, apart from the difference in analysis schemes, that the time-mean flows in the earlier investigations are representative of the wintertime average while the annual mean flow is used in the present study.

The present hemispheric energy cycle should be regarded as essentially reflecting extratropical energetics. Further investigations have been made of the energetics in the frequency domain in the following areas:

(i) Latitude-pressure distributions of energy parameters, with emphasis on the contrast between the extratropics and the tropics.

(ii) Interannual variability of energy conversions.

(iii) Intercomparison between energetics observed in the atmosphere and simulated in GCM experiments.

The results will be presented in a forthcoming paper (Sheng and Hayashi 1990).

Acknowledgments. The technical assistance of D. G. Golder is appreciated. One of the authors (J.S.) is indebted to Professor T. N. Krishnamurti for his encouragement and stimulating discussions on various aspects of this study. The authors are grateful to I. M. Held and N.-C. Lau for their comments on the original manuscript. The figures were drafted by the Scientific Illustration Group at GFDL.

APPENDIX A

Derivations of the Spectral Energy Equations for KE and APE

To obtain the equation for spectral KE, the equations of motion and continuity in a spherical-pressure coordinate system are written in flux form as

$$\frac{\partial u}{\partial t} = -\left[\frac{\partial}{\partial x}uu + \frac{\partial}{\partial y}vu + \frac{\partial}{\partial p}\omega u - \frac{\tan\phi}{a}uv\right] + 2\Omega\sin\phi v - g\frac{\partial z}{\partial x} + F_u, \quad \text{(A1)}$$

$$\frac{\partial v}{\partial t} = -\left[\frac{\partial}{\partial y}uv + \frac{\partial}{\partial y}vv + \frac{\partial}{\partial p}\omega v + \frac{\tan\phi}{a}uu\right] - 2\Omega\sin\phi u - \frac{g}{a}\frac{\partial z}{\partial\phi} + F_v, \quad \text{(A2)}$$

$$0 = -\left[\frac{RT}{p\theta}\right]\theta - g\frac{\partial z}{\partial p}, \quad \text{(A3)}$$

$$0 = \frac{\partial u}{\partial x} + \frac{\partial v}{\partial y} + \frac{\partial\omega}{\partial p}, \quad \text{(A4)}$$

where

$$\frac{\partial}{\partial x}(\ ) = \frac{1}{a\cos\phi}\frac{\partial}{\partial\lambda}(\ ), \quad \text{(A5)}$$

and

$$\frac{\partial}{\partial y}(\ ) = \frac{1}{a\cos\phi}\frac{\partial}{\partial\phi}\cos\phi(\ ). \quad \text{(A6)}$$

Taking the cospectrum operation between u and Eq. (A1) yields

$$0 = -\left[P_n\left(u, \frac{\partial}{\partial x}uu\right) + P_n\left(u, \frac{\partial}{\partial y}vu\right) + P_n\left(u, \frac{\partial}{\partial p}\omega u\right) - \frac{\tan\phi}{a}P_n(u, uv)\right] + 2\Omega\sin\phi P_n(u, v) - P_n\left(u, g\frac{\partial z}{\partial x}\right) + P_n(u, F_u). \quad \text{(A7)}$$

Similarly, the meridional momentum equation can be written as

$$0 = -\left[P_n\left(v, \frac{\partial}{\partial x}uv\right) + P_n\left(v, \frac{\partial}{\partial y}vv\right) + P_n\left(v, \frac{\partial}{\partial p}\omega v\right) + \frac{\tan\phi}{a}P_n(v, uu)\right] - 2\Omega\sin\phi P_n(v, u) - P_n\left(v, \frac{g}{a}\frac{\partial z}{\partial\phi}\right) + P_n(v, F_v). \quad \text{(A8)}$$

The spectral kinetic energy equation can be obtained by adding Eq. (A7) to Eq. (A8):

$$0 = \langle K\cdot K(n)\rangle + \langle A(n)\cdot K(n)\rangle + F(n) - D(n) \quad \text{(A9)}$$

where

$$\langle K\cdot K(n)\rangle = -\left[P_n\left(u, \frac{\partial}{\partial x}uu\right) + P_n\left(u, \frac{\partial}{\partial y}vu\right) + P_n\left(u, \frac{\partial}{\partial p}\omega u\right) + P_n\left(v, \frac{\partial}{\partial x}uv\right) + P_n\left(v, \frac{\partial}{\partial y}vv\right) + P_n\left(v, \frac{\partial}{\partial p}\omega v\right) - \frac{\tan\phi}{a}[P_n(u, uv) - P_n(v, uu)]\right], \quad \text{(A10)}$$

$$\langle A(n)\cdot K(n)\rangle = -P_n(\omega, \alpha), \quad \text{(A11)}$$

$$F(n) = -g\left[\frac{\partial}{\partial x}P_n(u, z) + \frac{\partial}{\partial y}P_n(v, z) + \frac{\partial}{\partial p}P_n(\omega, z)\right], \quad \text{(A12)}$$

$$D(n) = -[P_n(u, F_u) + P_n(v, F_v)]. \quad \text{(A13)}$$

In deriving Eq. (A9) the continuity equation (A4) and the hydrostatic equation (A3) have been used. Following Hayashi (1980), $\langle K\cdot K(n)\rangle$ can be further partioned into two parts as

$$\langle K\cdot K(n)\rangle = \langle K(m)\cdot K(n)\rangle + \langle K(0)\cdot K(n)\rangle. \quad \text{(A14)}$$

Here $\langle K(m)\cdot K(n)\rangle$ is the transfer of kinetic energy into frequency f_n by interactions among different frequencies excluding f_0 (time mean), while $\langle K(0)\cdot K(n)\rangle$ is the transfer of energy into frequency f_n by interaction between the mean flow and frequency f_n. By definition, $\langle K(m)\cdot K(n)\rangle$ is given by

$$\langle K(m)\cdot K(n)\rangle = -\left[P_n\left(u, \frac{\partial}{\partial x}u'u'\right) + P_n\left(u, \frac{\partial}{\partial y}v'u'\right) + P_n\left(u, \frac{\partial}{\partial p}\omega'u'\right) + P_n\left(v, \frac{\partial}{\partial x}u'v'\right) + P_n\left(v, \frac{\partial}{\partial y}v'v'\right) + P_n\left(v, \frac{\partial}{\partial p}\omega'v'\right) - \frac{\tan\phi}{a}[P_n(u, u'v') - P_n(v, u'u')]\right]. \quad \text{(A15)}$$

The equation for spectral APE is obtained by starting with the first law of thermodynamics:

$$\frac{\partial\theta}{\partial t} = -\frac{u}{a\cos\phi}\frac{\partial\theta}{\partial\lambda} - \frac{v}{a}\frac{\partial\theta}{\partial\phi} - \omega\frac{\partial\theta}{\partial p} + \left[\frac{\theta}{C_pT}\right]h. \tag{A16}$$

The potential temperature θ is split into an area mean and a departure, i.e.,

$$\theta = \{\theta\} + \theta^*. \tag{A17}$$

Substituting Eq. (A17) into Eq. (A16) gives

$$\frac{\partial\theta}{\partial t} = -\frac{u}{a\cos\phi}\frac{\partial\theta^*}{\partial\lambda} - \frac{v}{a}\frac{\partial\theta^*}{\partial\phi} - \omega\frac{\partial\theta^*}{\partial p} - \omega\frac{\partial\{\theta\}}{\partial p} + \left[\frac{\theta}{C_pT}\right]h. \tag{A18}$$

By using the continuity equation, (A18) can be written in the flux form:

$$\frac{\partial\theta}{\partial t} = -\frac{\partial}{\partial x}u\theta^* - \frac{\partial}{\partial y}v\theta^* - \frac{\partial}{\partial p}\omega\theta^* - \omega\frac{\partial\{\theta\}}{\partial p} + \left[\frac{\theta}{C_pT}\right]h. \tag{A19}$$

Following Lorenz (1955), Oort and Peixoto (1974) and Hayashi (1980), it is assumed that $\partial\{\theta\}/\partial p$ is time independent:

$$\frac{\partial\{\theta\}}{\partial p} = \frac{\partial\{\bar{\theta}\}}{\partial p}. \tag{A20}$$

Multiplying Eq. (A19) by $\gamma = (RT/p\theta)(-\partial\{\theta\}/\partial p)^{-1}$ and taking the cospectrum operation with θ, the equation for $A(n)$ is obtained as

$$0 = \langle A\cdot A(n)\rangle - \langle A(n)\cdot K(n)\rangle + G(n), \tag{A21}$$

where

$$\langle A\cdot A(n)\rangle = -\gamma\left[P_n\left(\theta, \frac{\partial}{\partial x}u\theta^*\right) + P_n\left(\theta, \frac{\partial}{\partial y}v\theta^*\right) + P_n\left(\theta, \frac{\partial}{\partial p}\omega\theta^*\right)\right], \tag{A22}$$

and

$$G(n) = \gamma\left[\frac{\theta}{C_pT}\right]P_n(\theta, h). \tag{A23}$$

Finally $\langle A\cdot A(n)\rangle$ is partitioned to give Eq. (4):

$$\langle A\cdot A(n)\rangle = \langle A(m)\cdot A(n)\rangle + \langle A(0)\cdot A(n)\rangle \tag{A24}$$

where

$$\langle A(m)\cdot A(n)\rangle = -\gamma\left[P_n\left(\theta, \frac{\partial}{\partial x}u'\theta^{*\prime}\right) + P_n\left(\theta, \frac{\partial}{\partial y}v'\theta^{*\prime}\right) + P_n\left(\theta, \frac{\partial}{\partial p}\omega'\theta^{*\prime}\right)\right]. \tag{A25}$$

APPENDIX B

List of Symbols

$A(n)$	available potential energy associated with frequency f_n
a	earth's radius
C_p	specific heat at constant pressure, 1004 J/(kg K)
$D(n)$	dissipation of kinetic energy associated with frequency f_n
f	frequency
f_n	discrete frequency of index n
F_u	frictional force in the x-direction
F_v	frictional force in the y-direction
$F(n)$	convergence of energy flux associated with frequency f_n
$G(n)$	generation of available potential energy associated with frequency f_n
g	gravitational force per unit mass, 9.81 N kg^{-1}
h	diabatic heating
$K(n)$	kinetic energy associated with frequency f_n
n	frequency index
P_n	frequency cospectrum
p	pressure
p_0	pressure constant, 1000 mb
R	gas constant, 287 J/(kg K)
T	temperature
t	time
u	eastward component of velocity
v	northward component of velocity
x	curvilinear coordinate toward the east
y	curvilinear coordinate toward the north
z	geopotential height
α	specific volume
γ	stability parameter
θ	potential temperature
λ	longitude
ϕ	latitude
Ω	angular velocity of the earth
ω	vertical pressure velocity
$\langle A(m)\cdot A(n)\rangle$	nonlinear transfer of APE into frequency f_n
$\langle A(0)\cdot A(n)\rangle$	transfer of APE from the time-mean motion into frequency f_n
$\langle A(n)\cdot K(n)\rangle$	conversion from APE to KE at frequency f_n
$\langle K(m)\cdot K(n)\rangle$	nonlinear transfer of KE into frequency f_n
$\langle K(0)\cdot K(n)\rangle$	transfer of KE from the time-mean motion into frequency f_n
$\{(\ )\}$	horizontal mean
$(\ )^*$	deviation from the horizontal mean
$\overline{(\ )}$	time mean
$(\ )'$	deviation from the time mean

REFERENCES

Bengtsson, L., M. Kanamitsu, P. Kallberg and S. Uppala, 1982: FGGE 4-dimensional data assimilation at ECMWF. *Bull. Amer. Meteor. Soc.*, **63**, 29–43.

Blackmon, M. L., J. M. Wallace, N.-C. Lau and S. L. Mullen, 1977: An observational study of the Northern Hemisphere wintertime circulation. *J. Atmos. Sci.*, **34**, 1040–1053.

——, Y. H. Lee and J. M. Wallace, 1984a: Horizontal structure of 500 mb height fluctuations with short, intermediate and long time scales. *J. Atmos. Sci.*, **41**, 961–979.

——, ——, —— and H. H. Hsu, 1984b: Time variation of 500 mb height fluctuations with long, intermediate and short time scales as deduced from lag-correlation statistics. *J. Atmos. Sci.*, **41**, 981–991.

Charney, J. G., 1971: Geostrophic turbulence. *J. Atmos. Sci.*, **28**, 1087–1095.

Chen, T. C., and A. Wiin-Nielsen, 1976: On the kinetic energy of the divergent and nondivergent flow in the atmosphere. *Tellus*, **28**, 486–498.

Dole, R. M., 1986: Persistent anomalies of the extratropical Northern Hemisphere wintertime circulation: Structure. *Mon. Wea. Rev.*, **114**, 178–207.

Green, J. S. A., 1977: The weather during July 1976: Some dynamic considerations of the drought. *Weather*, **32**, 120–128.

Hayashi, Y., 1980: Estimation of nonlinear energy transfer spectra by the cross-spectral method. *J. Atmos. Sci.*, **37**, 299–307.

——, 1987: A modification of the atmospheric energy cycle. *J. Atmos. Sci.*, **44**, 2006–2017.

——, and D. G. Golder, 1977: Space-time spectral analysis of mid-latitude disturbances appearing in a GFDL general circulation model. *J. Atmos. Sci.*, **34**, 237–262.

——, and ——, 1983: Transient planetary waves simulated by GFDL spectral general circulation models. Part II: Effects of nonlinear energy transfer. *J. Atmos. Sci.*, **40**, 951–957.

Holopainen, E. O., and C. Fortelius, 1987: High-frequency transient eddies and blocking. *J. Atmos. Sci.*, **44**, 1632–1645.

Hoskins, B. J., and D. Karoly, 1981: The steady linear response of a spherical atmosphere to thermal and orographic forcing. *J. Atmos. Sci.*, **38**, 1179–1196.

Illari, L., 1984: A diagnostic study of the potential vorticity in a warm blocking anticyclone. *J. Atmos. Sci.*, **41**, 3518–3526.

Julian, P., W. Washington, L. Hembree and C. Ridley, 1970: On the spectral distribution of large scale atmospheric kinetic energy. *J. Atmos. Sci.*, **27**, 376–387.

Kao, S. K., and H. N. Lee, 1977: The nonlinear interaction and maintenance of the large-scale moving-wave in the atmosphere. *J. Atmos. Sci.*, **34**, 471–485.

Kraichnan, R. H., 1967: Inertial ranges in two-dimensional turbulence. *Phys. Fluids*, **10**, 1417–1423.

Krishnamurti, T. N., P. K. Jayakumar, J. Sheng, N. Surgi and A. Kumar, 1985: Divergent circulations on the 30 to 50 daytime scale. *J. Atmos. Sci.*, **42**, 364–375.

Kung, E. C., 1988: Spectral energetics of the general circulation and time spectra of transient waves during the FGGE year. *J. Climate*, **1**, 5–19.

——, and H. Tanaka, 1983: Energetics analysis of the global circulation during the special observation periods of FGGE. *J. Atmos. Sci.*, **40**, 2575–2592.

Kuo, H.-L., 1949: Dynamical instability of two-dimensional nondivergent flow in a barotropic atmosphere. *J. Meteor.*, **6**, 105–122.

Lau, N.-C., 1988: Variability of the observed midlatitude cyclone tracks in relation to low-frequency changes in the circulation pattern. *J. Atmos. Sci.*, **45**, 2718–2743.

——, and E. O. Holopainen, 1984: Transient eddy forcing of the time-mean flow as identified by geopotential tendencies. *J. Atmos. Sci.*, **41**, 313–328.

Leith, C. E., 1968: Diffusion approximation for two dimensional turbulence. *Phys. Fluids*, **11**, 671–673.

——, 1971: Atmospheric Predictability and two-dimensional turbulence. *J. Atmos. Sci.*, **28**, 145–161.

Lorenz, E. N., 1955: Available potential energy and the maintenance of the general circulation. *Tellus*, **7**, 157–167.

——, 1967: The nature and theory of the general circulation of the atmosphere. World Meteorological Organization, Geneva, 161 pp.

——, 1969: The predictability of a flow which possesses many scales of motion. *Tellus*, **21**, 289–307.

——, 1979: Forced and free variations of weather and climate. *J. Atmos. Sci.*, **36**, 1367–1349.

Madden, R. A., and P. R. Julian, 1971: Detection of a 40–50 day oscillation in the zonal wind in the tropical Pacific. *J. Atmos. Sci.*, **28**, 702–708.

——, and ——, 1972: Detection of global-scale circulation cells in the tropics with a 40–50 day period. *J. Atmos. Sci.*, **29**, 1109–1123.

Manabe, S., J. Smagorinsky, J. L. Holloway, Jr. and H. M. Stone, 1970: Simulated climatology of a general circulation model with a hydrological cycle. *Mon. Wea. Rev.*, **98**, 175–212.

Miyakoda, K., J. Sheldon and J. Sirutis, 1982: Four-dimensional analysis experiment during the GATE period. Part II. *J. Atmos. Sci.*, **39**, 486–506.

Mullen, S. L., 1987: Transient eddy forcing of blocking flows. *J. Atmos. Sci.*, **44**, 3–22.

Oort, A. H., 1964: On estimates of the atmospheric energy cycle. *Mon. Wea. Rev.*, **92**, 483–493.

——, and J. P. Peixoto, 1974: The annual cycle of the energetics of the atmosphere on a planetary scale. *J. Geophys. Res.*, **79**, 2705–2719.

Saltzman, B., 1957: Equations governing the energetics of the large scales of atmospheric turbulence in the domain of wave number. *J. Meteor.*, **14**, 513–523.

——, 1970: Large-scale atmospheric energetics in the wave number domain. *Rev. Geophys. Space Phys.*, **8**, 289–302.

Savijarvi, H. I., 1977: The interaction of the monthly mean flow and large-scale transient eddies in two different circulation types. Part II: Vorticity and temperature balance. *Geophysica*, **14**, 207–229.

Sheng, J., 1986: On the energetics of low frequency motions. Ph.D. dissertation, Florida State University, 171 pp.

——, and Y. Hayashi, 1990: Observed and simulated energy cycles in the frequency domain. *J. Atmos. Sci.*, **47**, 1243–1254.

Simmons, A. J., J. M. Wallace and G. W. Branstator, 1983: Barotropic wave propagation and instability, and atmospheric teleconnection patterns. *J. Atmos. Sci.*, **40**, 1363–1392.

Smagorinsky, J., 1972: The general circulation of the atmosphere. *Meteorological Challenges: A History*, D. P. McIntyre, Ed., 338 pp.

Tanaka, H., 1985: Global energetics analysis by expansion into three-dimensional normal mode functions during the FGGE winter. *J. Meteor. Soc. Japan*, **63**, 180–200.

Vinnichenko, N. K., 1970: The kinetic energy spectrum in the free atmosphere—1 second to 5 years. *Tellus*, **22**, 158–165.

Wallace, J. M., and N.-C. Lau, 1985: On the role of barotropic energy conversion in the general circulation. *Adv. Geophys.*, **28A**, 33–74.

Wiin-Nielsen, A., 1962: On transformation of kinetic energy between the vertical shear flow and the vertical mean flow in the atmosphere. *Mon. Wea. Rev.*, **90**, 311–320.

——, 1967: On the annual variation and spectral distribution of atmospheric energy. *Tellus*, **19**, 540–559.

Wilson, M. A. G., 1975: A wavenumber-frequency analysis of large-scale tropospheric motions in the extratropical Northern Hemisphere. *J. Atmos. Sci.*, **32**, 478–488.

Yasunari, T., 1980: A quasi-stationary appearance of 30 to 40 day period in the cloudiness fluctuations during the summer monsoon over India. *J. Meteor. Soc. Japan*, **58**, 225–229.

——, 1981: Structure of an Indian summer monsoon system with around 40-day period. *J. Meteor. Soc. Japan*, **59**, 336–354.

Zangvil, A., 1977: On the presentation and interpretation of spectra of large-scale disturbances. *Mon. Wea. Rev.*, **105**, 1469–1472.